

# POTENTIAL AND SHORTCOMING OF SMALL SATELLITE FOR TOPOGRAPHIC MAPPING

Rainer Sandau

DLR, German Aerospace Center, Rutherfordstr. 2, 12489 Berlin, Germany  
phone +49 30 67055 530, fax +49 30 67055 532, rainer.sandau@dlr.de

Commission I WG I/6

**KEYWORDS:** Photogrammetry, Remote Sensing, Mapping, Digital, Camera, Small/micro satellites, High resolution, Spatial

## ABSTRACT:

High resolution mapping systems follow the trend to smaller ground sample distances (GSD) making use of the best technology available at the given time. From the 80 m GSD of ERTS in 1972, the GSD now approached 1 m and even less for civil applications. Mass and power consumption of spacecrafts and imaging instruments follow similar trends in conjunction with the immense improvements in very divers fields of technology. SAR systems are an alternative to passive optical systems; they also benefit from the technology improvements. But the most promising prospects for high resolution mapping with small satellites are connected with passive optical systems. The paper gives a MTF based metrics and analytical method to assess how far we can go with decreasing instrument size and decreasing the GSD at the same time and what features the spacecraft needs to provide. In this context the paper deals with such important parameters for topographic mapping with small satellites like spatial resolution, radiometry, pointing accuracy and stability. It is shown that the imagers as well as the spacecraft bus need to follow certain rules to allow high resolution imaging aboard of small satellites.

## 1. INTRODUCTION

High resolution mapping systems follow the trend to smaller ground sample distances (GSD). Figure 1 shows this trend for civil Earth surface imagers using passive optical approaches. The increasing number of spaceborne imaging systems in the last decade (see [1] for more) shows that an increasing number of countries is dealing with spaceborne technology and that there is an increasing need for mapping systems for different applications [2]. The trend to smaller GSDs was and is supported by the improvements in diverse fields of technology as for instance optics, mechanics and materials, electronics, signal processing, communication and navigation. The spaceborne mapping systems always attempted to achieve the highest ground resolution possible with the available technology at a given time. Also mass, volume and power consumption of the spacecrafts and the instruments followed the trend to miniaturization. Active micro wave systems, e. g. SAR systems, are an alternative to passive optical mapping systems. They also benefit from the technology improvements. But the most promising prospects for high resolution mapping with small satellites are connected with passive optical systems, especially push-broom systems. High resolution optical systems on small satellites have to overcome a couple of problems. In this paper we consider a GSD of 10 m or less as high resolution, and a satellite with 1000 kg or less mass as small satellite (see table 1) according to the IAA Study Cost-Effective Earth Observation Missions [3].

Smaller GSD needs larger focal lengths. The physics behind optical systems allows only a restricted number of tricks to overcome the problems of large focal length optics in terms of volume and mass. The size of the focal plane depends on the detector system size and is part of the equation concerning

large satellites	$\geq 1000$ kg
small satellites	
- mini satellites	< 1000 kg
- micro satellites	< 100 kg
- nano satellites	< 10 kg
- pico satellites	< 1 kg

Table 1 Classification of small satellites [3]

optics volume and mass. The pointing stability is said to be too low using small satellites. What are the requirements and restrictions. The large amounts of data of high resolution imaging systems need to be stored and transmitted using high performance devices. Size, mass and power consumption of those devices increase with increasing data volumes and data rates. High resolution means also to deal with small amounts of energy coming from small ground pixels to be registered in small integration time periods according to the high satellite orbit velocities. So, the question is how far can we go with decreasing the GSD (increasing the ground resolution) using small satellites.

## 2. TOPOGRAPHIC MAPPING CONCEPTS

There are several possibilities to perform topographic mapping, most of them can make use of line or matrix technologies.

- 1) Across-track stereo (see fig. 2) due to side viewing feature (e. g. SPOT-1 – SPOT-4)
- 2) Along-track stereo
- 2.1) 1 sensor concept using forward/backward slewing feature (see fig. 3)

Phase 1 imaging in forward slewing mode  
 Phase 2 imaging in backward slewing mode  
 (e. g. IKONOS, EarlyBird (matrix camera), QuickBird)

- 2.2) 2 sensor concept using forward/backward looking sensors with
  - 2 cameras, e. g. HRS on SPOT-5
  - 2 line arrays of a single camera, e. g. OPS on JERS1, ASTER on Terra (see fig. 4)
- 2.3) 3 sensor concept using forward/nadir/backward sensors with
  - 3 cameras, e. g. MOMS-02 on STS-55 and MIR/Priroda
  - 3 line arrays of a single camera, e. g. WAOSS-B on BIRD (see fig. 5).

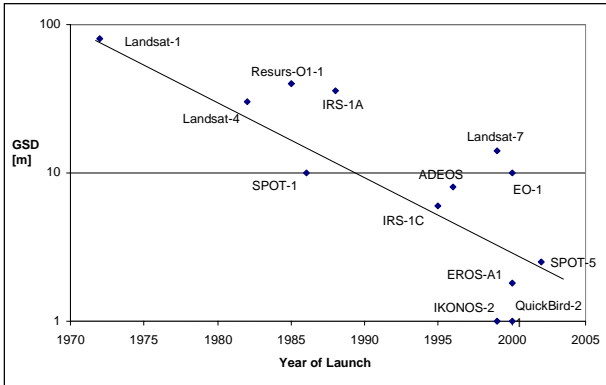


Figure 1 Some civil Earth surface imagers, trend of GSD

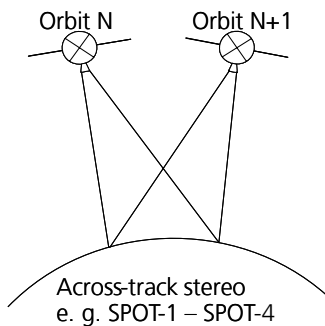


Figure 2 Across-track stereo principle

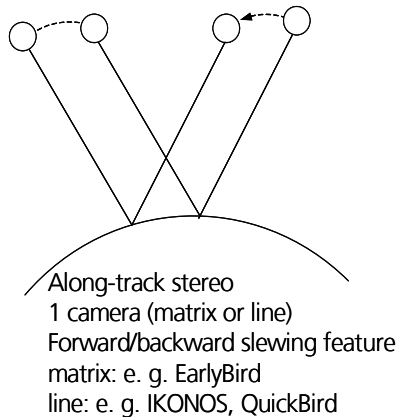
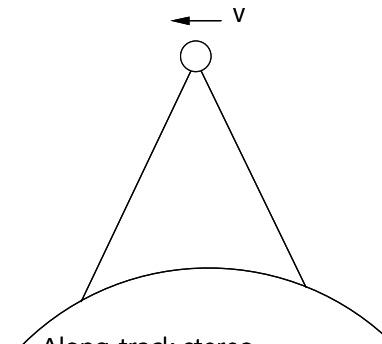
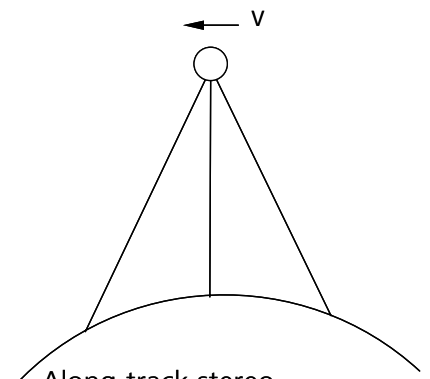


Figure 3 Along-track stereo using the slewing feature of the satellite or platform



Along-track stereo  
 2 lines on 1 FPA / camera or  
 2 single line cameras  
 1 camera: e. g. OPS of JERS-1  
 2 cameras: e. g. HRS of SPOT-5

Figure 4 Along-track stereo with 2 sensors



Along-track stereo  
 3 lines on 1 FPA (e. g. WAOSS) or  
 3 single line cameras (e. g. MOMS-02)

Figure 5 Along-track stereo with 3 sensors

### 3. IMPORTANT PARAMETERS FOR SPACEBORNE MAPPING SYSTEMS

In this chapter only some major features are described and a few suggestions are given to support miniaturization in order to come in the range for small satellite designs.

#### 3.1 Spatial resolution

Some major features are considered which influence the image quality from the spatial resolution point of view. A very effective way to describe the image quality is to use the Modulation Transfer Function MTF. Using the MTF approach, you can multiply all the image quality influencing MTF components of a linear system (or quasi linear system) which may base on different physical effects (e. g. optics, CCD, electronics, ...) in order to create the system MTF. The resulting point spread function PSF of the system is then computed applying the Inverse Fourier Transform (IFT). For simplicity we use here

$$MTF_{SR} = MTF_{Optics} \cdot MTF_D \cdot MTF_{PS} \quad (1)$$

(SR – spatial resolution, D – detector, PS – platform stability)

The  $MTF_{PS}$  of the platform stability is subject of chapter 3.3.  $MTF_{Optics}$  includes the diffraction part as well as the aberration part.

For most of the operating systems, the optical system may be considered near diffraction limited and in focus. For a diffraction limited circular aperture of optics, the  $MTF_{Optics}$  can be described with

$$MTF_{Optics}(f_x, f_y) = \left[ \frac{2}{\pi} \left[ \arccos\left(\lambda \frac{f}{D} f\right) - \lambda \frac{f}{D} f \sqrt{1 - \left(\lambda \frac{f}{D} f\right)^2} \right] \right] \quad (2)$$

for  $\lambda \frac{f}{D} f \leq 1$

with  $f$  the focal length,  $D$  the aperture diameter of the optics,  $\lambda$  the average wavelength of the radiation, and  $f = \sqrt{f_x^2 + f_y^2}$ . This diffraction causes a diffraction disc or Airy disc.

The Airy disc diameter  $d$  caused by diffraction is derived from  $PSF_{Optics}$  (see[9]). It is one of the important parameters which can be related to the detector pixel size  $x$

$$d = 2.44 \cdot \lambda \cdot \frac{f}{D} = 2.44 \cdot \lambda \cdot F \quad (3)$$

with  $f$  the focal length,  $D$  the aperture of the optics, and  $\lambda$  the average wavelength of the radiation. If  $x$  is larger than  $d$  the system is detector limited, the resolution is determined by the detector. Otherwise the optics determines the spatial resolution. Figure 6 shows the borderline for an average wavelength of  $\lambda = 0.55 \mu m$  (green). The optics designs should be near to the borderline on the optics limited side in order to get maximum energy for the detector avoiding too large aliasing effects. For state-of-the-art CCD detectors with a pitch of  $7 \mu m$ , an  $f/5.2$  optics would satisfy this approach.

$MTF_D$  of the detector element with size  $d$  is described by the sinc function

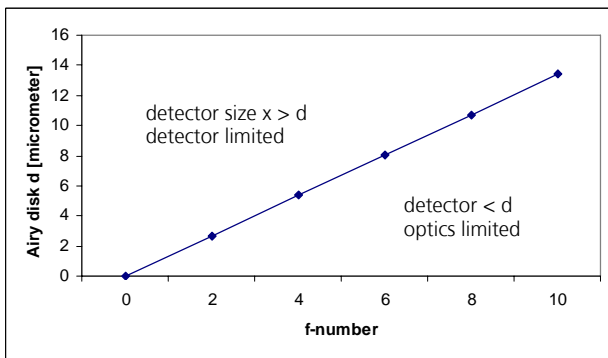


Figure 6 Airy disk parameter  $d$  as a function of the f-number  $F$  ( $\lambda=0.55 \mu m$ )

$$MTF_D(f_x) = \sin c(d \cdot f_x) = \frac{\sin c(d \cdot f_x)}{d \cdot f_x} \quad (4)$$

Fig. 7 gives an impression of the relations for an CCD pixel size of  $x = 10 \mu m$  behind an  $f/1.2$  optics.

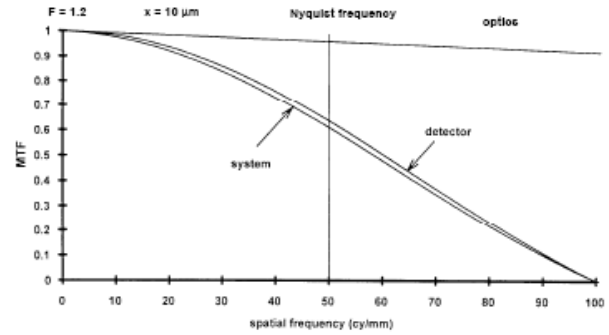


Figure 7 System MTF composed of  $MTF_{Optics}$  and  $MTF_D$

### 3.2 Radiometric aspects

The number of photoelectrons generated in a solid state camera is

$$n_{pc} = \frac{A_D \cdot T_{Optics} \cdot t_{int}}{4F^2} \int_{\lambda_1}^{\lambda_2} R_d(\lambda) L(\lambda) d\lambda \quad (5)$$

( $A_D$  – detector area,  $T_{Optics}$  – transmission of the optics,  $t_{int}$  – integration time,  $F$  –f-number,  $R_d$  – detector responsivity,  $L$  – radiation flux) with  $t_{int} < t_{dwell}$ .

Once the detector is selected,  $A_D$  and  $R_d$  are given.  $L$  is also given as well as  $F$  and  $T_{Optics}$  when the optics is selected or designed taking into account the technological and/or the mission constraints.  $\Delta\lambda$  is fixed in most cases, so that the only real variable part is the integration time  $t_{int}$ . For a satellite in LEO, the satellite ground track velocity is about  $7 \text{ km/s}$ . In other words, the dwell time is  $1 \text{ ms}$  for a ground sample distance GSD of  $7 \text{ m}$ . For high resolution imagers with GSD of about  $1 \text{ m}$ ,  $t_{int} < 1/7 \text{ ms}$  is too short for a sufficient good signal and SNR.

$$t_{dwell}(1m) / t_{dwell}(10m) = 1/10 \quad (6)$$

Even more severe is the influence of the pixel field of view (IFOV).

$$IFOV(1m) / IFOV(10m) \cong 1/100 \quad (7)$$

Taking both aspects into account, reducing the GSD by a factor of  $10^1$  causes a time related and geometry related decrease of energy at the detector of about  $10^{-3}$ .

There are two possibilities to overcome this obstacle:

- use TDI (Time Delay and Integration) technology with N stages in order to increase the signal N-fold and improve the SNR by the factor of  $\sqrt{N}$  (this technique is used e. g. in the IKONOS and QuickBird missions)
- use the so-called slow-down mode in order to decrease the ground track velocity of the line projection on the surface (those technique is used for instance in the EROS-A1 mission) with respect to the satellite velocity in order to obtain the necessary dwell time  $t_{\text{dwell}}$ .

### 3.3 Pointing stability

There are many activities going on to develop and test instruments, actuators, and algorithms to control the pointing with high accuracy. The obtained accuracies are between arcseconds and fractions of degrees. For mapping of the Earth's surface, deviations from the necessary precisions can be corrected using precise ground control points. The pointing stability is of more importance in order to maintain the ground sample distance and the image quality. The  $MTF_{\text{PS}}$  of the platform has three major components

$$MTF_{\text{PS}} = MTF_{\text{LM}} \cdot MTF_{\text{J}} \cdot MTF_{\text{sin}} \quad (8)$$

(PS – platform stability, J – jitter, sin – sinusoidal vibration)

The MTF degradation due to linear motion of the satellite is

$$MTF_{\text{LM}}(f_x) = \text{sinc}(a_{\text{LM}} \cdot f_x) \quad (9)$$

where  $f_x$  is the spatial frequency, and  $a_{\text{LM}}$  the distance the target edge moves across the detector pixel.  $MTF_{\text{LM}}$  only affects the MTF in the direction of the motion. The distance  $a_{\text{LM}}$  is  $v \cdot \Delta t$ . In many cases  $\Delta t$  is close to the dwell time and  $MTF_{\text{LM}}$  is approximately  $MTF_{\text{D}}$ . Fig. 8 shows the influence of  $a_{\text{LM}}$  on the  $MTF_{\text{LM}}$ .  $MTF_{\text{LM}}$  with  $a_{\text{LM}} = 1$  equals the detector  $MTF_{\text{D}}$ . The abscissa shows the spatial frequency normalized to the system

dependend maximum value  $f = \frac{f_x}{f_{x,\text{max}}}$ . For instance, with a

detector pitch of  $6.5 \mu\text{m}$  the spatial frequency of  $150 \text{ cyc/mm}$  equals  $f_i = 1$ . As a rule-of-the-thumb, when the linear motion causes an image shift less than about 20 % of the detector size, the effect on system performance is minimal.

For  $MTF_{\text{J}}$  (jitter or random motion) is assumed that the jitter is a superposition of different high-frequency motions so that the central limit theorem can be applied. It says that many random movements can be described by a Gaussian distribution

$$MTF(f_j) = \exp(-2\pi^2 \sigma_j^2 f_j^2) \quad (10)$$

with  $\sigma_j$  the rms random displacement. Fig. 9 shows the influence of  $\sigma$  on the  $MTF_{\text{J}}$  for  $\sigma = 0.1 \cdot x$  and  $\sigma = 1 \cdot x$  ( $x$  – detector element size).

As a rule-of-the-thumb, when  $\sigma_j$  is less than about 10 % of the detector size  $x$ , system performance is only minimal effected. Attitude control systems for pointing accuracies and

stabilization to support high resolution functions on micro satellites are under development. In some cases, disturbing vibrations may also be avoided by simply switching off the active control functions during the relatively short imaging phase.

A sinusoidal platform vibration is to be considered for systems with larger integration times (lower ground resolution) using

$$MTF_{\text{sin}}(f_x) = J_0(2\pi a_{\text{sin}} f_x) \quad (11)$$

$$t_{\text{int}} \gg \frac{2\pi}{\omega}$$

( $J_0$  – Bessel function of order zero,  $a_{\text{sin}}$  – amplitude of sinus wave)

Fig. 9 shows the influence of the amplitude  $a$  of a sinusoidal platform vibration. As a rule-of-the-thumb, when the amplitude  $a$  is less than 10 % of the pixel size, the effect on system performance is minimal.

Fig. 11 shows the degradation of the detector  $MTF_{\text{D}}$  (with detector size  $x$ ) due to the influence of  $MTF_{\text{PF}}$  when for all three components of  $MTF_{\text{PF}}$  the rule-of-the-thumb parameters are applied ( $MTF_{\text{LM}}$  with  $a_{\text{LM}} = 0.2 \cdot x$ ,  $MTF_{\text{J}}$  with  $\sigma = 0.1 \cdot x$ ,  $MTF_{\text{sin}}$  with  $a = 0.1 \cdot x$ ). The resulting  $MTF_{\text{pfi}}$  equals  $MTF_{\text{SR}}$  with neglected  $MTF_{\text{optics}}$  ( $MTF_{\text{optics}} = 1$ ).

From an orbit altitude of 600 km, a GSD of 1 m equals an IFOV of  $1.7 \mu\text{rad}$  or approximately  $1/3$  of an arcsec. During the dwell time, the drift shall be less than 20 % of the IFOV resulting in a drift rate of about 2.4 mrad/s or 8 arcmin/s in order to stay in the limit for minimal degradation of the MTF due to drift effects. When using the TDI principle to improve the SNR, for a 96 step TDI the tolerable drift rate becomes even  $25 \mu\text{rad/s}$  or about 5 arcsec/s!

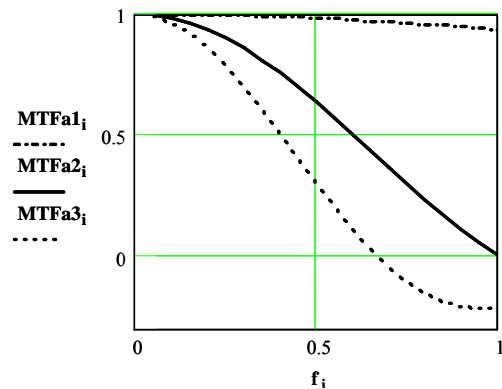


Figure 8 Influence of  $a_{\text{LM}}$  on  $MTF_{\text{LM}}$  with  $a_{\text{LM}} = 0.1, 1, 1.5 \cdot \text{GSD}$

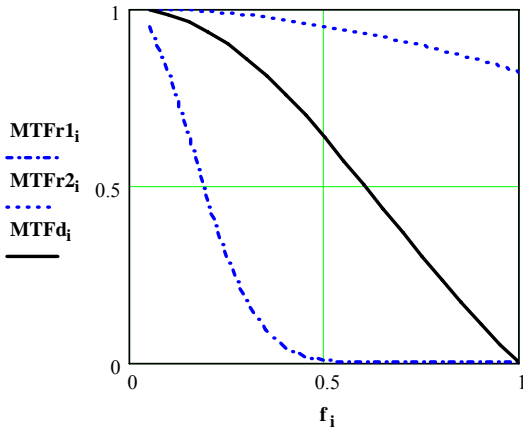


Figure 9 Influence of  $s$  on the  $MTF_J$  with  $s = 0.1, 1 \cdot x$ . For comparison,  $MTF_D$  is also shown ( $MTF_d$ ).

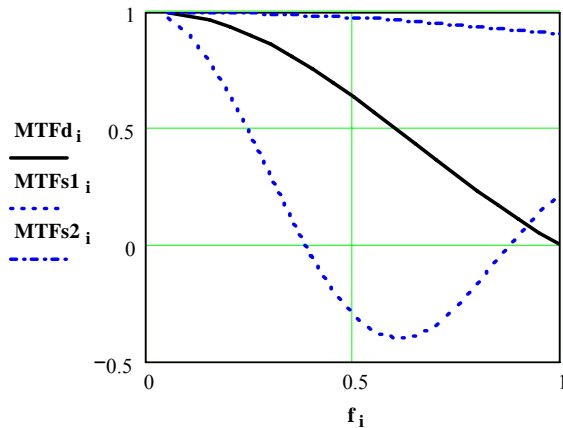


Figure 10 Influence of the amplitude  $a$  of a sinusoidal vibration on  $MTF_{sin}$  with  $a = 0.1, 1 \cdot x$ . For comparison,  $MTF_D$  is also shown ( $MTF_d$ ).

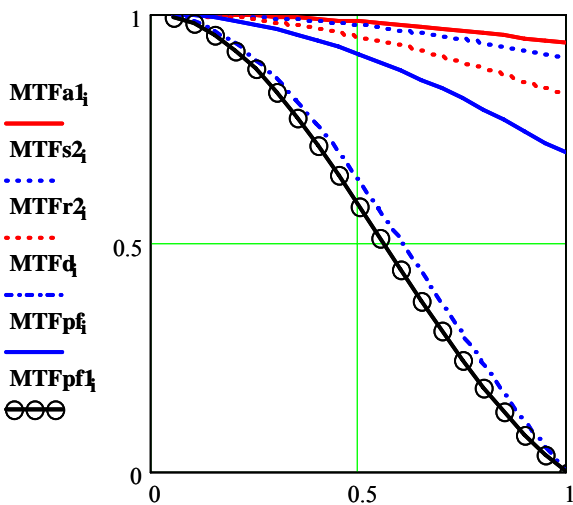


Figure 11 Degradation of detector  $MTF_D$  ( $MTF_d$ ) due to  $MTF_{PS}$  ( $MTF_{pf}$ ) consisting of  $MTF_{LM}$  ( $a = 0.2 \cdot x$ ),  $MTF_J$  ( $\sigma = 0.1 \cdot x$ ),  $MTF_{sin}$  ( $a = 0.1 \cdot x$ ). Resulting  $MTF$  is  $MTF_{pfl}$ .

### 3.4 Data volume & transmission rate

Data rate is a very important parameter for imagers on small satellites. Most small satellites use X-Band transmitters allowing up to 100 MBit/s. The ground station contact time from LEO is about 10 minutes resulting in roughly 60 GBit to be transmitted. If no compression is applied, a quadratic image of 87 kByte x 87 kByte can be transmitted during the ground station contact time. Whatever is used, the store & dump mode or the real-time mode, careful planning of the orbit activities is of high importance to make most use of this bottleneck.

Kn band transmission systems are developed now which allow band widths up to 1 GBit/s with smaller antennas, that is less mass and volume.

### 3.5 Mass, Volume, Power Consumption

**3.5.1 Microelectronics:** Since the launch of Landsat-1 in 1972, the progress in microelectronics enabled more sophisticated instrument designs. The developments for the MESUR Network Mission may serve as an example, how much microelectronics technology may influence the overall mission design. The MESUR (Mars Environmental Survey) Network Mission concept consisted of up to 16 small spacecraft (that time planned to be launched in 2001). As often in extraterrestrial missions, there was a pressure to miniaturization by need. Reference mission was the MESUR Pathfinder Mission, one of the first missions under NASA's Discovery program of smaller, low-cost missions to be launched 1997.

In [3] the benefits have been assessed which may occur when the electronics technology used in the MESUR Pathfinder mission is replaced by advanced microelectronics technology. The MESUR Network study team found out that advanced microelectronics packaging technologies could be applied to the implementation of subsystem functions for

- the Attitude and Information Management System AIMS
- the Radio Frequency Subsystem RF
- the Power and Pyro Subsystem PP.

As a result, a factor of three or better reduction in mass, volume, and power consumption were projected relative to the MESUR Pathfinder baseline (see table 2).

The key to realize these reductions lies in the utilization of industry-based advanced microelectronics packaging technologies, including:

- multichip module (MCM) technology
- three-dimensional MCM stacking
- Die stacking for memory.

	Pathfinder	Network	Net Reduction	Fractional
Mass	47 kg	11 kg	36 kg	4.3 x
Volume	46 dm <sup>3</sup>	6.5 dm <sup>3</sup>	39.5 dm <sup>3</sup>	7.1 x
Power	74 W	26 W	49 W	2.9 x

Table 2 Projected total reduction in mass, volume, and power consumption for MESUR Network in comparison to MESUR Pathfinder

The leverage of these reductions to the spacecraft is obvious. The advanced microelectronics packaging technologies have been widely used for instance in a joint NASA/DLR study for the ROSETTA lander carrying among other cameras a stereo camera with 10 mm GSD [5] and in a joint DLR/NASA three-

line stereo camera concept for planetary exploration [6]. The effects have been remarkable. The latter concept resulted for instance in very small stereo camera for a GSD of 20 m and a swath width of 250 km from an orbit altitude of 250 km, and with a weight of 2 kg and a power consumption of 12.5 Watts including a 1 Gbit mass memory.

**3.5.2 Detector: Pixel size influence** - For mapping purposes the pixel size of the detector is projected via the focal length to the ground pixel size to be obtained, the smaller the detector elements  $x$  the shorter the focal length  $f$  (see figure 12). As an example, the state-of-the-art CCD pixel size of  $7\mu\text{m}$  results in a focal length of  $f = 4.2$  m. Of course with smaller detector sizes less energy is integrated. If the sensitivity of the pixel element is not sufficient to obtain the necessary SNR, TDI needs to be applied or a so called slow-down mode allows to enlarge the dwell time to the sufficient extent (should not be used in stereo imaging).

Impact of staggered configurations - Volumes and mass of an optics depends significantly on the focal length and the aperture, but also on the image field size determined by the detector extensions. Using staggered line arrays (see fig. 13), the following effects occur:

- detector line length is halved
- image field area is reduced to one quarter
- focal length is halved
- the optics need to be of high quality for twice as many line pairs per millimeter with respect to the line pairs per millimeter necessary for the pixel size.

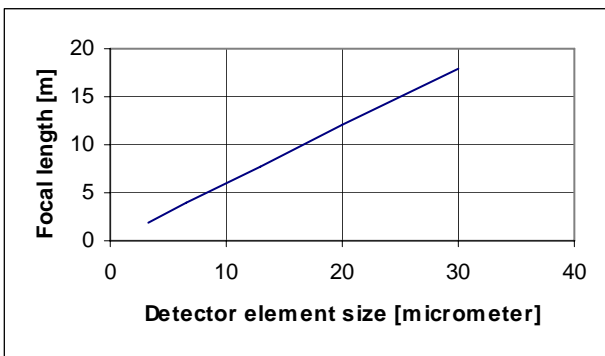


Figure 12 Dependence between detector element size  $x$  and necessary focal length  $f$  for a given ground pixel size of  $X = 1$  m from an orbit altitude of 600 km

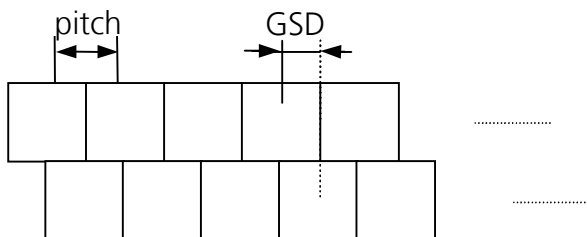


Figure 13 Staggered linear detector array configuration

Staggered CCD-line arrays are used for instance in the SPOT-5 mission cameras HRS.

**3.3.3 Optics:** The focal length of high resolution space born sensors is determined by the physics laws and seems to be in contradiction to a small satellite concept in terms of mass and volume. The progress in production and test of optic systems enables now the utilization of highly efficient low-mass and low-volume optical telescopes for space applications. Examples are

- Use of aspheric lenses in refractive telescopes
- Use of folded arrangements for reflective telescopes (e. g. TMA)
- Use of sophisticated catadioptric telescopes.

Even if you can design a camera having weight compatible with a micro-satellite spacecraft, the volume of the lens system for high resolution space-borne imagers is a problem if you think of the restricted size envelope for piggy-back launch opportunities.

The Technical University of Berlin recently performed a study concerning an interesting optics construction approach: the Dobson Space Telescope, DST, [7]. The core element of DST is a  $20''$   $f/5$  Newton telescope. The secondary mirror will be placed via four 2.1 m booms when the spacecraft is already in orbit. In order to fulfill micro satellite requirements it is folded to minimal space during the launch. This type of telescopes called truss design Dobson was originally invented by ambitious amateur astronomers. To increase the resolution for remote sensing purposes, a "Barlow lens" with a factor of 2.5 pushes the focal ratio up to  $f/12.5$  which assures maximum possible magnification and a ground pixel size of about 1m from a 700 km orbit.

#### 4. OUTLOOK

This paper showed the problems connected with high resolution topographic imaging. But it showed also the possibilities resulting from the immense improvements in many fields of technology. So it is not surprising that there are a good number of small satellites (total mass  $< 500$  kg) with high-resolution instruments ( $\leq 10$  m GSD) in orbit or planned. Table 3 shows the missions which have no stereo capabilities.

Mission	GSD [m]	Launch
Earth Observation-1/NASA	10 m	2000
HIT-1/China	10 m	2004
FORMOSAT-2/Taiwan	2 m	2004
PROBA/ESA	5 m	2001
DMC/China	4 m	2005
X-SAT/ Singapore	10 m	planned
EKOSAT-IR/Germany, Israel, Korea	5 m	planned
MAC/ Korea, Malaysia	2.5 m	planned
MSMI/ South Africa	2.5 m	planned
DST/ Germany	1 m	planned

Table 3 Small satellite high resolution mapping missions, without stereo capabilities

The suite of small satellite mission in orbit or planned for topographic mapping is smaller (see table 4).

From the technology point of view small satellite missions for topographic mapping are feasible. Table 4 shows that even a GSD of less than 1 m is attacked. Once the performance concerning data quality for mapping is proven, there is a chance to install mapping systems with a low cost space segment. When we restrict ourselves to civil applications, the market will show whether or not those systems can compete with SPOT-5 topographic maps (GSD of 5 m).

On the higher resolution side, those systems will compete with the standard aerial photography market. If for some reasons high-resolution maps with worldwide high repetition rates are required, the necessary coverage asks for many cost-effective systems. Then there is a high need to install more cost-effective small satellite-based systems for mapping.

Mission	GSD [m]	Launch
EROS-A1/ Israel	1.8 m	2000
TOPSAT/ UK	2.5 m	2005
EROS-B/ Israel	0.82 m	2005
Rapid Eye/ Germany	6.5 m	planned
Diamant-1/ Germany	5 m	planned

Table 4 Topographic mapping missions with small satellites

## REFERENCES

- [1] Kramer, H. J., *Observation of the Earth and its environment – survey of missions and sensors*, Springer Verlag Berlin, Heidelberg, New York, 2002, 4 Ed.
- [2] Konecny, G., *Geoinformation – remote sensing, Photogrammetry and geographic information systems*. London and New York: Taylor & Francis., 2003
- [3] Cost-Effective Earth Observation Missions, IAA Study, Taylor & Francis The Netherlands, in print
- [4] Alkalai, L.; Davidson, J. (Eds.), MESUR Network – Integrated Microelectronics Study. Final Report, JPL D-11192, January 7, 1994
- [5] Sandau, R.; Alkalai, L., ROSETTA – Surface Science Package – Integrated Microelectronics Study. DLR-FB 94-29, 1994
- [6] Sandau, R.; Hilbert, S.; Venus, H.; Fang, W.-C.; Alkalai, L., “A Three-Line Stereo Camera Concept for Planetary Exploration”, Paper IAA-L-0902 of the 2nd International Conference on Low-Cost Planetary Missions, April 16-19, 1996, Laurel, Maryland, USA
- [7] Segert, T.; Danziger, B.; Geithner, M., “The Dobson Space Telescope – A time shared Telescope for NEO and Earth Observation”, Paper IAA-B4-0605 of the 4th International IAA Symposium on Small Satellites for Earth Observation, April 7-11, 2003, Berlin, German
- [8] Jacobsen, K.: High Resolution Satellite Imaging Systems – an Overview, PFG 6/2005, 487-496
- [9] Jahn, H.; Reulke, R., *Systemtheoretische Grundlagen optoelektronischer Sensoren*, Akademie Verlag, Berlin, 1995